Full Tensor SQUID Gradiometer for airborne exploration

A Chwala
IPHT Jena
A Einstein Str 9
07745 Jena Germany
andreas.chwala@ipht-jena.de

R Stolz
IPHT Jena
A Einstein Str 9
07745 Jena Germany
ronny.stolz@ipht-jena.de

V Zakosarenko
IPHT Jena
A Einstein Str 9
07745 Jena Germany
zakosarenko@ipht-jena.de

L Fritzsch
IPHT Jena
A Einstein Str 9
07745 Jena Germany
ludwig.fritzsch@ipht-jena.de

M Schulz
IPHT Jena
A Einstein Str 9
07745 Jena Germany
marco.schulz@ipht-jena.de

A Rompel
Anglo Technical Services
45 Main Street
2001 Johannesburg South Africa
ARompel@angloamerican.co.za

L Polome
Spectrem Air Limited
PO Box 457
1748 Lanseria South Africa
louis@spectrem.co.za

M Meyer
Supracon AG
Wildenbruchstr 15
07745 Jena Germany
meyer@supracon.com

H G Meyer
IPHT Jena
A Einstein Str 9
07745 Jena Germany
meyer@ipht-jena.de

SUMMARY

IPHT Jena and Supracon AG develop and fabricate full tensor magnetic gradiometer (FTMG) systems, based on low-temperature-superconducting (LTS) planar-type SQUID (Superconducting Quantum Interference Device) gradiometers of first order. The systems are operated by Spectrem Air Ltd., jointly owned by Anglo American and De Beers. This paper describes details of the system setup, data processing and achieved performance parameters.

The sensors work at 4.2 K in liquid helium. With a base length of only 3.5 cm a real gradient measurement is possible. With six gradiometer the full magnetic gradient tensor can be measured with redundancy, allowing for high system reliability and the application of enhanced noise reduction techniques.

The data of the FTMG system will allow for a 3D inversion for the underlying magnetic sources. Examples of 2D maps of tensor components with high spatial resolution are shown.

Key words: SQUID, Gradiometry, Potential Fields, Mineral Exploration

INTRODUCTION

The airborne mapping of the Earth's magnetic field is widely used for geophysical exploration. The main limitation for directional magnetic field sensors was the overwhelming motion noise in the Earth's magnetic field. Therefore, only the total magnetic intensity (TMI) is measured. Nowadays often the so called horizontal or vertical gradients of the TMI are measured, but due to the long base length of these gradiometers (typically between 2 and 15 m) which is of the same order as the distance to the sources these measures are rather magnetic field differences than gradients. Furthermore, these "gradients" don't bear the same information content as the magnetic gradient tensor components, really measuring directional derivatives of the magnetic field:

$$\hat{G} = (G_{IK}) = \frac{\partial B_I}{\partial x_K} = \begin{pmatrix} G_{XX} & G_{XY} & G_{XZ} \\ G_{YX} & G_{YY} & G_{YZ} \\ G_{ZX} & G_{ZY} & G_{ZZ} \end{pmatrix} \quad (1).$$

We have to assume

$$\begin{aligned} div(\vec{B}) &= 0 \\ rot(\vec{B}) &= 0 \end{aligned} \quad (2),$$

if no currents are flowing in the surface. Therefore the tensor is fully described by five independent components as it is symmetric and the trace is zero:

$$\hat{G} = (G_{IK}) = \frac{\partial B_I}{\partial x_K} = \begin{pmatrix} G_{XX} & G_{XY} & G_{XZ} \\ & G_{YY} & G_{YZ} \\ & & \end{pmatrix} \quad (3).$$

Starting in 1997, we have developed a SQUID based system that measures the tensor components directly. Schmidt and Clark (2000) have shown that such a measurement has many advantages compared to conventional TMI measurements.

SYSTEM SETUP

The planar-type LTS SQUID gradiometers and reference magnetometers are based on standard all-refractory $Nb/AlO_X/Nb$ technology developed at IPHT in Jena (Stolz 1999). They are waterproof and robust against thermal cycling. The gradiometers have pick-up loop areas of 2.5 cm × 2 cm and they are connected in series. The pick-up loops are inductively coupled to a second order gradiometer SQUID.

The six planar-type SQUID gradiometers and four SQUID magnetometers are mounted on the bottom of a cryostat, a thermally insulated non-magnetic container which is filled with liquid helium. The nonlinear SQUID characteristic is linearized by a feedback circuit on top of the cryostat, which

enables a high system bandwidth and dynamic range. The analogue SQUID signals are digitized at a sampling rate of 1 kHz using extremely high-sensitive and low-drift 24bit AD converters.
The data acquisition unit also incorporates the batteries for up to 10 hours operation, a Novatel GPS board, an inertial measurement unit (three accelerometers and fiber optical gyroscopes), a pressure regulator and an interface to an external radar altimeter. Cryostat and data acquisition are mounted in an aerodynamically designed non-magnetic bird, which is towed by a helicopter, see figure 1. Data are transferred via wireless connection (WLAN) or glass fibre interface to a laptop on board the helicopter, where all system parameters can be monitored during flight. The data recording software tool also incorporates the calculation of the positions for the navigation system of the pilot.

Figure 1: Non-magnetic bird towed below a helicopter on a 20 m long rope.

DATA PROCESSING

The data processing stream is visualized in figure 2.

The first step is the synchronization of all data streams in the data acquisition system followed usually by a decimation to a 10 Hz data rate.

The common mode rejection, the rate of suppression of a homogeneous magnetic field by the sensor, of our gradiometers is on the order of 10^4 limited by the lithographic precision (approximately 300 nm) of the production tools. This results in a raw gradiometer signal which is a superposition of the measured tensor component and a sum of the measured magnetic field components by three parasitic pickup areas, which are presented by the balancing coefficients. Therefore, after the calibration of the data a procedure called balancing has to be done in the post-processing. It calculates the real gradient by subtracting the product of the magnetometer readings (B_X, B_Y, and B_Z) and the balancing coefficients α_K from each gradiometer signal:

$$G = G_{measured} - \alpha_x B_x - \alpha_y B_y - \alpha_z B_z \quad (4).$$

The coefficients α_k are calculated by a least squares algorithm, minimizing the standard deviation of G. After balancing we typically achieve a common mode rejection of 10^7 to 10^8 by this means. In this algorithm we assume in principle that there are no geomagnetic gradients. Improvements of this procedure which have to take into account locally and regionally existing magnetic gradients will be reported later. Figure 3 illustrates the importance of the balancing.
Next step is the extraction of the tensor components from the mixed measurements of the planar-type gradiometers. As the gradiometers measure directional components of the tensor it is necessary to rotate the measured gradient tensor from the body coordinate system into an Earth fixed coordinate system, in our case ENU (East-North-Up) by use of the attitude angles, namely the Euler angles, which are calculated by an extended Kalman filter, based on the measured accelerations, angular rates and GPS readings.

RESULTS

One very important parameter of each system is the noise limited resolution in flight. Currently, we achieve a rms noise floor of < 10 pT/m for all gradiometer channels after balancing in a 4.5 Hz bandwidth in low turbulence. Figure 4 shows the noise for different lines at high and low altitude for all gradiometers after balancing and another simple denoising step. While we can assume there are almost no gradients at high altitude, the estimated noise floor at low altitudes is of course contaminated by gradients originated from geology and artificial sources.

The FTMG systems have been tested over various targets. We selected as example the mapping of geologic structures in the Bushveld complex in Mpumalanga province, South Africa. This survey has been flown in 2006. Figure 5 shows the full magnetic gradient tensor of 7 km x 7 km area. For comparison reasons, the tensor component G_{ZZ} is also show (which is in fact just $-G_{xx}-G_{yy}$). It is clearly visible, that different geological features are more pronounced by different tensor components which act as directional filters.

REFERENCES

Schmidt, P.W. and D.A. Clark, Advantages of measuring the magnetic gradient tensor. Preview, 85, p. 26-30, 2000.

R. Stolz, L. Fritzsch, and H.-G. Meyer, LTS SQUID sensor with a new configuration, Superconductor Science and Technology, Vol. 12, pp. 806-808, 1999.

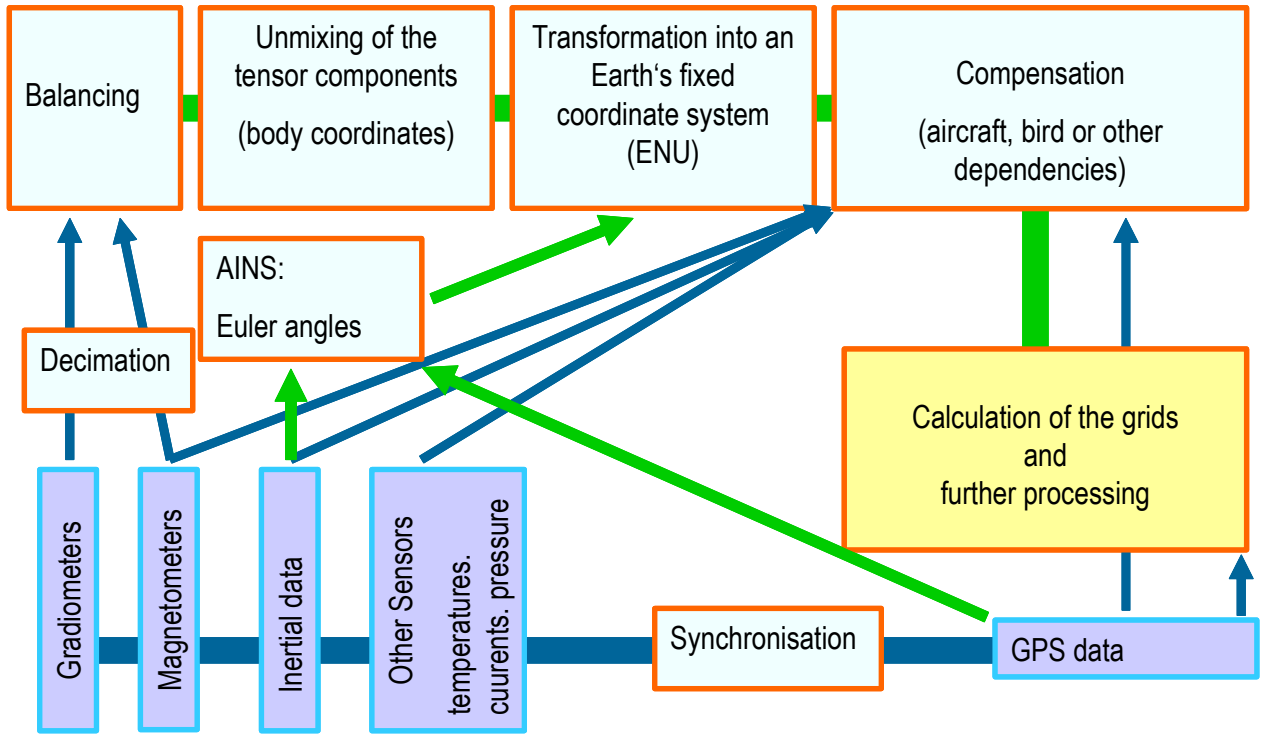

Figure 2: Processing stream: from raw data (purple) to compensated data in the Earth reference frame (yellow).

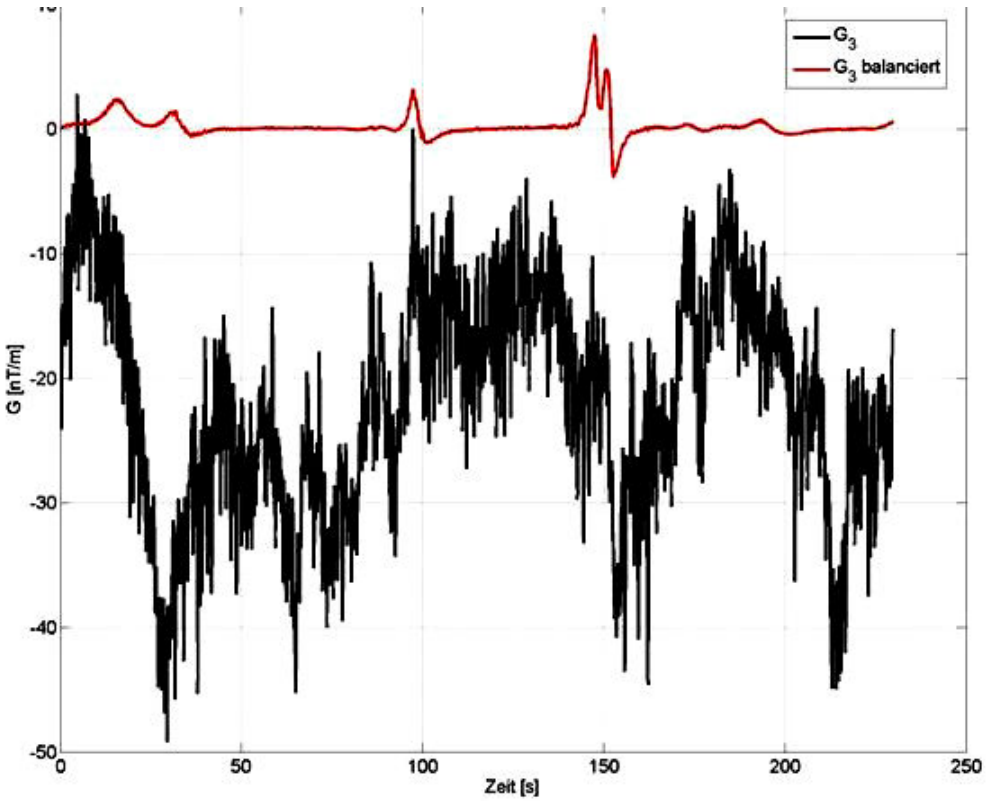

Figure 3: Comparison of raw gradiometer data (black) and balanced gradiometer data (red).

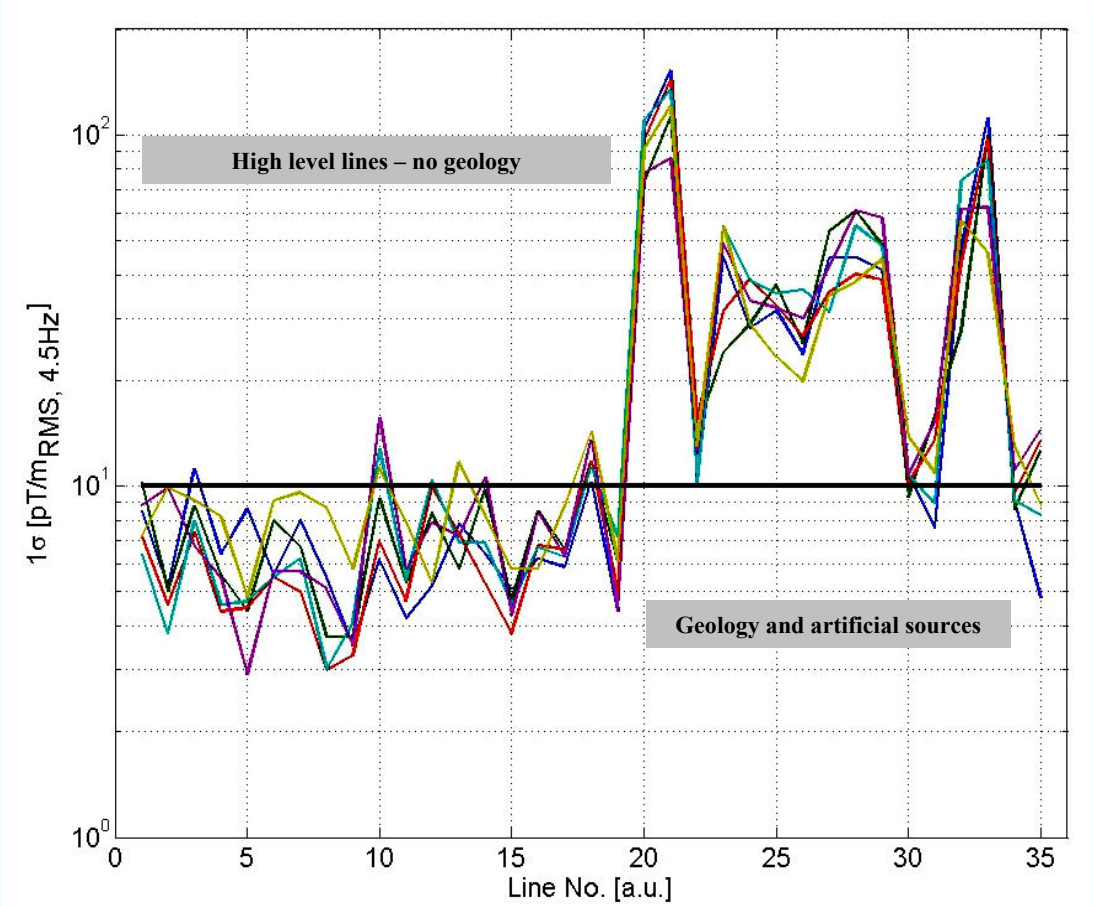

Figure 4: RMS noise for different lines of a survey for all 6 gradiometer channels after balancing and a simple compensation for high level lines (Line No. <20, Line 34, 35) and survey lines (Line No. from 200 to 33). Each colour represents one gradiometer.

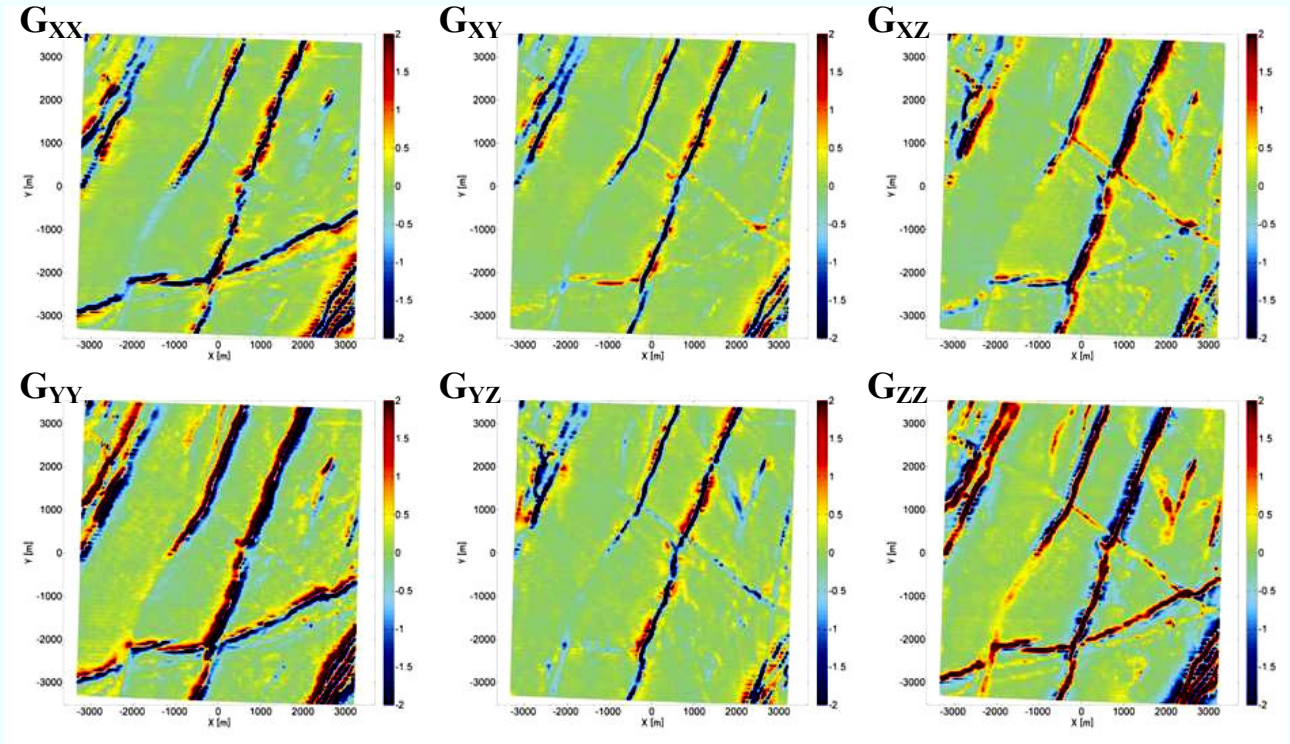

Figure 5: Full magnetic gradient tensor.